



Fracture toughness testing of small ceramic discs and plates

Stefan Strobl^{a,b}, Stefan Rasche^b, Clemens Krautgasser^{a,b}, Eugenia Sharova^{a,b}, Tanja Lube^{b,*}

^a Materials Center Leoben Forschung GmbH, Roseggerstraße 12, 8700 Leoben, Austria¹

^b Institut für Struktur- und Funktionskeramik, Montanuniversität Leoben, Peter-Tunner-Straße 5, 8700 Leoben, Austria²

Received 3 December 2013; accepted 14 December 2013

Available online 6 January 2014

Abstract

A new fracture toughness test for discs and plates is presented, which can be applied to small specimens (>5 mm diameter). A semi-elliptical surface crack is made into the centre of the top plane using a Knoop indenter. Then the layer containing the plastically deformed zone is ground off and the crack is loaded in tension using the Ball-on-3-Balls test.

Applied to five different ceramic materials the results gained with the new method agree well with those of standardised methods.

© 2013 Elsevier Ltd. All rights reserved.

Keywords: Fracture toughness; Mechanical characterisation; B3B; B3B-KIc; Surface Crack in Flexure

NOTICE:

This is the author's version of a work that was accepted for publication in the Journal of the European Ceramic Society. Changes resulting from the publishing process, such as peer review, editing, corrections, structural formatting, and other quality control mechanisms may not be reflected in this document. Changes may have been made to this work since it was submitted for publication.

A definitive version was subsequently published in
Journal of the European Ceramic Society 34 (2014) 1637-1642
doi: 10.1016/j.jeurceramsoc.2013.12.021

Fracture toughness testing of small ceramic discs and plates

Stefan Strobl^{a,b}, Stefan Rasche^b, Clemens Krautgasser^{a,b}, Eugenia Sharova^{a,b},
Tanja Lube^{b,*}

^a Materials Center Leoben Forschung GmbH, Roseggerstraße 12, 8700 Leoben,
Austria^c

^b Institut für Struktur- und Funktionskeramik, Montanuniversität Leoben, Peter-
Tunner-Straße 5, 8700 Leoben, Austria^d

* Corresponding author at: Institut für Struktur- und Funktionskeramik, Montanuniversität
Leoben, Peter-Tunner-Straße 5, 8700 Leoben, Austria.

Tel.: +43 3842 402 4111; fax: +43 3842 402 4102.

E-mail address: tanja.lube@unileoben.ac.at (T. Lube).

^c mclburo@mcl.at, <http://www.mcl.at>.

^d isfk@unileoben.ac.at, <http://www.isfk.at>.

Keywords:

Fracture toughness; mechanical characterization; B3B; B3B-KIc; Surface Crack in Flexure;

Abstract

A new fracture toughness test for discs and plates is presented, which can be applied to small specimens (>5 mm diameter). A semi-elliptical surface crack is made into the centre of the top plane using a Knoop indenter. Then the layer containing the plastically deformed zone is ground off and the crack is loaded in tension using the Ball-on-3-Balls test.

Applied to five different ceramic materials the results gained with the new method agree well with those of standardised methods.

1. Introduction

Cylindrical disc specimens are a favourable geometry if new materials are developed or materials are prepared in laboratory scale, e.g. by uniaxial pressing or by hot pressing. Disc

shaped specimens are also used for biaxial strength testing of dental materials [1] or zirconia for surgery [2].

Apart from this, many ceramic bulk components have the shape of thin discs or plates. Examples are ceramic membranes [3], (heat generating) resistors [4], capacitors [5], low temperature co-fired ceramics [6, 7] (LTCC), microchips [8, 9], piezoelectric speakers [10], watchcases and glasses [11] or armour ceramics [12, 13] and much more.

Mechanical properties may depend on the processing route. Therefore it is suitable to determine these properties on real components and not on specially produced bodies. For that reason and to save costs for special specimen production it may be beneficial to use the components directly as specimens and to test mechanical properties on thin discs or plates [14-18].

The most common biaxial test assemblies are listed in [19] and disadvantages such as unclear contact situation are discussed. The ball-on-3-balls test [20] (B3B) was recently developed to overcome all these aspects. In this test, the plates are supported by 3 balls on one side and loaded by a fourth ball in the centre of the opposite side. Hence, the maximum tensile stress occurs at the surface of the plate directly opposite to the centre ball. Based on this idea discs and rectangular plates have also successfully been tested [6-9, 21-23]. For sake of clarity, the principle of the B3B is explained here for symmetrically loaded discs, see Fig. 1. The test piece (i.e. the disc) is defined by its radius R and thickness t . The three balls with radius R_B are in contact with each other; therefore the loading radius R_a is given by the relation $R_a = (2/\sqrt{3}) R_B$.

The flexural strength is the maximum tensile stress, σ_{B3B} , in the specimen during loading, given by [19]:

$$\sigma_{B3B} = \frac{F}{t^2} f\left(\frac{R_a}{R}, \frac{t}{R}, \nu\right) \quad (1)$$

with the maximum load at failure F , the disc thickness t , and a dimensionless factor f , which depends on the geometry of the specimen and on the Poisson's ratio ν of the tested material, etc. Values for that function can be found in [24]. The calculation of σ_{B3B} for discs can also easily be performed with an interactive Web-Mathematica tool at our homepage <http://www.isfk.at/en/960/>.

Due to the well-defined stress field and low measurement uncertainties [25], the B3B is a good basis for fracture toughness testing. In analogy to the standardized “Surface Crack in Flexure” (SCF) method [26, 27] a semi-elliptical surface crack is used as starter crack in the centre of the disc. This new method is further called B3B-KIc and is presented in this work.

2. Modelling the B3B test with a surface crack

In this new method a surface crack is created in the centre of the disc on the surface opposite to the loading ball (i.e. the position of the maximum stress σ_{B3B} in the conventional B3B test). This is done using a Knoop indenter analogously to the Surface Crack in Flexure (SCF) method [26, 27]. Underneath of the indent the material is plastically deformed, which causes residual stresses. These stresses may conflict the measurement. To remove these residual stresses a surface layer of the plates (discs) containing the plastically deformed zone has to be ground off. Following the SCF standard [26, 27] the required minimum thickness of this surface layer to be removed can be estimated; an even more accurate advice is given in [28].

The stress distribution in the conventional B3B test has a three-fold symmetry [19] (see Fig. 2a). Therefore, it is not possible to achieve a symmetrical loading of the semi-elliptical crack, even if the crack is perfectly centred in the stress field. As illustrated in Fig. 2b the stress intensity on the left and the right hand side of the crack differ. For this reason we introduce the convention that one crack tip has to be directed towards one contact point of a supporting ball, see Fig. 2b. The consequences of errors originating from this kind of positioning (Fig. 2c) are discussed later.

The crack is approximated to be perfectly semi-elliptical, where a is the crack depth and $2c$ is the full crack width at the surface (a and c correspond to the semi-axes of the ellipse). A more complete analysis of the influence of the exact crack shape on fracture toughness evaluation can be found in [28].

The fracture toughness K_{Ic} is given by to the following equation:

$$K_{Ic} = \sigma_{B3B} Y \sqrt{a \pi} \quad , \quad (2)$$

whereas Y is the geometric factor that depends on the geometry of crack and specimen and on the Poisson’s ratio of the material. The calculation of Y was performed using the commercial finite element program package ANSYS Workbench, version 13, and a J -integral

formulation; for details see [29]. The maximum of Y along the crack front was evaluated in the linear elastic approach. The FE model is built up parametrically. The geometric factor is a function of the following four dimensionless parameters:

$$Y = Y\left(\frac{a}{c}, \frac{a}{t}, \frac{t}{R_a}, \nu\right) \quad (3)$$

The influence of these dimensionless parameter intervals were evaluated for a wide range of geometries and materials (through the influence of the Poisson ratio ν), which cover most of the practical possible needs:

- relative disc thickness: $0.05 \leq t/R_a \leq 0.35$
- relative crack depth: $0.01 \leq a/t \leq 0.4$
- crack shape: $0.5 \leq a/c \leq 1$
- Poisson's ratio: $0.1 \leq \nu \leq 0.4$

The influence of the disc radius (or the ratio R_a/R , respectively) on the geometric factor can be neglected (the variation of Y is smaller than 0.25 % for $0.5 \leq R_a/R \leq 0.95$). Thus, no special evaluation is necessary to obtain Y for rectangular plates by using the appropriate R_a .

The trend of $Y(a/c, a/t)$ for a representative set of dimensionless parameters ($t/R_a = 0.35$ and $\nu = 0.3$) is illustrated in Fig. 3. In all analysed cases Y decreases with the relative crack depth a/t . This is reasonable considering that for a constant crack shape, the surface points of the crack are further away from the disc centre with the maximum tensile stress. The deepest point of the semi-elliptical crack approaches the region of compressive stresses. The maximum of the geometric factor along the crack front was used for an interpolation function (i.e. used for data evaluation).

3. Experimental

The new B3B-KIc method was tested on five different types of ceramics: alumina, LTCC bulk material, silicon carbide, silicon nitride and barium titanate. For all materials the fracture

toughness was also determined with conventional standardised methods (SEVNB [30] and/or with the SCF method [26, 27]).

- a) The investigated material (Rubalit 708S) is a commercial 96% alumina substrate ceramic produced by CeramTec AG, Germany. It was delivered in form of laser-cut circular discs with as-sintered surfaces (diameter 8 mm, thickness ~ 0.6 mm) [31]. The bending bars ($20 \times 2 \times 1.6 \text{ mm}^3$) for SEVNB testing were also laser-cut from similar plates.
- b) The silicon carbide (EKasic F) was provided by ESK Ceramics GmbH & Co. KG (Kempten, Germany) and has an average grains size of $< 5 \mu\text{m}$. The discs had a diameter of 20.6 mm and a thickness of 3.1 mm. Miniature bars ($13 \times 2 \times 1.5 \text{ mm}^3$) machined from the discs were used for SEVNB testing.
- c) The LTCC material, referred to as MKE, was provided in the as-sintered state by TDK-EPC (Deutschlandsberg, Austria). It consists of Al_2O_3 particles (approx. 40 vol. % with a mean diameter of $2 \mu\text{m}$) embedded in a silicate based glass matrix. Microstructural characterisation of the material can be found in previous work [6, 7] Rectangular plates with $10 \times 11 \times 1 \text{ mm}^3$ were used for B3B-KIc testing. Small bar specimens ($20 \times 3 \times 1 \text{ mm}^3$) machined from similar plates were used for SEVNB testing.
- d) The barium titanate material (PTC, positive temperature coefficient resistors) is a classical functional ceramic used for thermistors [4, 32] and was provided by (TDK-EPC Corporation, Deutschlandsberg, Austria). Generally, barium titanate is not linear-elastic, which was neglected for this investigation. As-sintered discs with 19.4 mm diameter and a thickness of ~3 mm were used, whereas the bending bars ($40 \times 4 \times 3 \text{ mm}^3$) were machined from bulk material.
- e) The investigated silicon nitride (FSNI) is a commercial hot pressed material provided by FCT Ingenieurkeramik (Rauenstein, Germany). As a sintering aid and for improvement of the mechanical properties overall ~10 wt. % Al_2O_3 and Y_2O_3 were used; it has a grain size of 1-10 μm [33]. Discs (diameter 19.2 mm and thickness 1.7 mm) as well as bars ($40 \times 4 \times 3 \text{ mm}^3$) were machined from the same plate material.

The preparation procedure of the specimens of all materials was generally the same: Fixation of several discs on a planar plate with glue – polishing to uniform thickness – indentation (and infiltration of penetration dye) – measurement of the indent size and initial crack size – calculation of grinding depth – grinding-off of the surface layer – removal of the specimens from the plate and cleaning in acetone – measurement of thickness of the discs and the full crack width $2c$ at the surface.

In principle this approach is relatively fast for the production of a fracture toughness specimen, if the material is initially given in the form of discs. In the case of LTCC no penetration dye was used but – to facilitate the measurement of the initial crack size on the fracture surface – the Knoop indents were introduced with a tilt of 3° from the disc axis [26, 27].

A universal testing machine (Zwick Z010, Zwick GmbH & Co. KG, Ulm, Germany) was used for load application. The tests were performed using a sufficient crosshead speed to achieve fracture within 5 to 10 seconds.

After testing the crack shape of the pre-crack was measured on both fracture surfaces and the average values of a and c , respectively, were calculated. One representative example for a crack in each material is shown in Fig. 4. It depends on the material and the crack size, if (fluorescentic) penetration dye is needed for an accurate determination of the crack geometry.

4. Results and discussion

Due to the dimensionless formulation (eq. 3) of the geometric factor it is possible to test specimens in a broad range of parameters and material types. The assumed Poisson's ratios and the mean values and standard deviation of the measured specimen and crack geometries as well as the K_{Ic} results of the B3B-KIc test are given in Table 1. The data evaluation was conducted according to eq. 2. In each case at least four specimens were tested.

In all cases the mean values of the K_{Ic} results are typical values for the investigated types of ceramics. The highest value was obtained for FSNI with $5.0 \pm 0.3 \text{ MPa m}^{1/2}$ and the lowest for the PTC material with $1.4 \pm 0.1 \text{ MPa m}^{1/2}$.

In the last column of Table 1 the results of the fracture toughness $K_{Ic,alternative}$ evaluated with SEVNB and/or SCF are shown for comparison. In the most cases the fracture toughness K_{Ic} matches $K_{Ic,alternative}$ very well within the standard deviation. For MKE and PTC the alternative SEVNB method deliver slightly lower results compared to B3B-KIc.

This may happen in materials with R-curve behaviour due to the small cracks at the notch tip for SEVNB [34].

The scatter of the achieved plate thicknesses, crack depth and crack width is very small, which indicates a good reproducibility of the specimen preparation (of course each specimen was evaluated separately). Therefore, it is not surprising that the K_{Ic} results have a low scatter. The standard deviation of the K_{Ic} values is about 10 % for MKE and less than 6 % for

all other materials. The standard deviation obtained with the new B3B-KIc method is in the same range of standardised methods for fracture toughness determination.

5. Error analysis

All previously presented results were evaluated for a perfectly centred and horizontally aligned crack (see Fig. 2b). Due to the fact that the region of maximum stress is very localized, the influence of small deviations of the crack alignment on the measured value is analysed. For the error analysis a reference model with the following parameters is assumed: $R = 10$ mm, $t = 2$ mm, $R_B = 7.5$ mm, $\nu = 0.3$, $a = 100$ μm and $2c = 300$ μm (i.e. $a/c = 0.66$, $a/t = 0.05$, $t/R_a = 0.23$). This corresponds approximately to the parameters of the FSNI specimens. The resulting error due to measurement errors of the crack geometry is assumed to be similar to that for the conventional SCF method. It has been pointed out in several works [35-37].

Considering the strong localisation of the maximum stress and the three-fold symmetry in the B3B, the alignment of the crack in the centre of the disc is a crucial point for the practical accuracy of the B3B-KIc method. For a perfectly centred and aligned crack the stress intensity factor at the deepest point of the crack is approximately 3 % higher compared to that at the surface point of the crack (this situation is generally preferable for surface cracks in flexure [28, 35]).

For the error analysis three possible deviations from the ideal crack position can be separated: lateral offset in x or y direction (i.e. Δx and Δy) and an inclination (see Fig. 2c). Deviations from the ideal geometry of less than 30° in the inclination angle and less than 150 μm offset from the centre seem easily to be feasible in practice. If a centred crack is inclined, the resulting error in Y is less than - 0.2 % for all directions (0° to 90°). Therefore, for this specific crack and specimen geometry the influence of the inclination angle on the measured value is negligible.

In the case of a lateral offset, the whole crack or at least one side of the crack is farther away from the position of the maximum tensile stress σ_{B3B} (position (0,0), see Fig. 2c). But for a maximum offset in x-direction of 150 μm ($\hat{=} c$) the other crack tip is exactly in the centre (at the position of σ_{B3B}). Considering a lateral offset of $\Delta x = \pm 150$ μm , $\Delta y = 0$ and an inclination angle $\pm 30^\circ$, the worst case of error in Y is - 0.7 % . Note that Y is always

lowered due to the increasing distance from the position of maximum stress. A similar calculation for $\Delta y = \pm 150 \mu\text{m}$ and $\Delta x = 0$ results in an error of less than -1% .

Considering the worst case combination of lateral positioning errors (within $\Delta x = \Delta y = \pm 150 \mu\text{m}$ and maximum inclination angle of $\pm 30^\circ$) the geometric factor decreases by max. 2% . All positioning errors lead to an overestimation of the K_{Ic} value.

Hence, for practical crack positioning, it is recommended to ensure two points: i) the offset has to be small related to the loading radius R_a (3% or less) and ii) the offset has to be equal or less than c . Furthermore, a crack shape ratio of approximately $a/c = 0.66$ (or less) should be used, so that the stress intensity factors at the surface and in depth are (at least) equal.

As mentioned before the influence of the ratio R_a/R on the geometric factor can be neglected in discs. Therefore, it is assumed that generally the shape of the plates (circular, rectangular, etc.) does not much affect the results of the geometric factor. Note that also for rectangular B3B specimens the preparation procedure and the calculation of Y remains the same, only the calculation of σ_{B3B} has to be modified. For this reason the B3B-KIc method is very flexible in practice regarding preparation as well as data evaluation.

It was also mentioned that “small” specimens can be tested, so what is the lower limit of specimen size? The B3B as a strength test was already applied to thin plates with diameters of about 1.5 mm [21-23]. Consequently, it depends on the material, whether suitable cracks (shape and relative depth) can be induced by a Knoop indenter. For small cracks (related to R_a), the stress field is almost constant over the whole crack and the only obvious restriction for a small crack is the worst case positioning error (i.e. offset). Assuming a minimum crack width of $c = 50 \mu\text{m}$, it should be ensured that the offset is less than $50 \mu\text{m}$ (equal to c). Errors resulting from inclination of the crack can be neglected.

An upper limit for the crack width c is given by the maxima of the evaluated parameter ranges. A rough guideline is $c/R_a \leq 0.25$. For a large, shallow crack the deepest point of the crack is always the critical point. Therefore positioning errors of large cracks (e.g. $c = 500 \mu\text{m}$), a positioning error – e.g. offset $50 \mu\text{m}$ – would almost not affect the results.

Considering all practical aspects (crack measurement, indent and specimen positioning, grinding artefacts and parallelism of the plates) it is estimated that the lower limit of the disc diameter is about 5 mm . In any case, shallow cracks ($a/c \leq 0.66$ and $a/t \leq 0.1$) have to be

preferred to keep measurement errors low, especially for small specimens. Generally, thicker specimens are easier to handle [38], but care has to be taken to ensure a valid geometry (t/R) for the B3B test [19, 24].

6. Conclusions

A new fracture toughness test for discs and rectangular plates is presented, which is also applicable to small specimens. FE calculations of the geometry factor Y were performed within a wide range of practically relevant parameters. The dimensionless formulation of the geometric factor enables a very flexible specimen preparation and simple evaluation of experiments. Different sources of measurement error were considered and discussed regarding specimen and crack size. Five different ceramic materials were tested using the B3B-K_{Ic} method. The obtained K_{Ic} results match very well the results determined with the alternative methods. The main conclusions are:

- The most important source of error is the lateral offset of the crack from the centre of the specimen.
- The influence of inclination of the crack can be neglected for typical crack/specimen geometries.
- Specimens with diameters down to 5 mm can be tested with an estimated overall measurement error below 5 %.
- The scatter of the K_{Ic} results is comparable with that of standardized fracture toughness testing methods.
- The specimen preparation and testing procedure is economical and simple to perform.

It has been shown that this new method is applicable to several structural and functional ceramics. Therefore, we expect a high capability for characterization of brittle materials, including small components or biomaterials, e.g. human teeth.

Literature

[1]. ISO 6872. Dentistry — Ceramic materials. 2008.

- [2]. ISO 13356. Implants for surgery — Ceramic materials based on yttria-stabilized tetragonal zirconia (Y-TZP). 2008.
- [3]. Minh NQ. Ceramic Fuel Cells. *Journal of the American Ceramic Society* 1993;76:563-88.
- [4]. Röhrig S, Supancic P. New Self-regulating Ceramic PTC Thermistor Heating Elements with Strongly Improved Performance. *Ceramic Forum International* 2012;89:E25-E9.
- [5]. Carlson T, Asp LE. Structural carbon fibre composite/PET capacitors – Effects of dielectric separator thickness. *Composites Part B: Engineering* 2013;49:16-21.
- [6]. Bermejo R, Supancic P, Aldrian F, Danzer R. Experimental approach to assess the effect of metallization on the strength of functional ceramic components. *Scripta Materialia* 2012;66:546-9.
- [7]. Bermejo R, Supancic P, Krалева I, *et al.* Strength reliability of 3D low temperature co-fired multilayer ceramics under biaxial loading. *Journal of the European Ceramic Society* 2011;31:745-53.
- [8]. Deluca M, Bermejo R, Pletz M, *et al.* Strength and fracture analysis of silicon-based components for embedding. *Journal of the European Ceramic Society* 2011;31:549-58.
- [9]. Deluca M, Bermejo R, Pletz M, *et al.* Influence of deposited metal structures on the failure mechanisms of semiconductor components. *Journal of the European Ceramic Society* 2012;32:4371-80.
- [10]. Roh Y, Moon C. Design and fabrication of an ultrasonic speaker with thickness mode piezoceramic transducers. *Sensors and Actuators A: Physical* 2002;99:321-6.
- [11]. Isler P. Watches: Mechanical Materials. In: *Encyclopedia of Materials: Science and Technology (Second Edition)*. Buschow KHJ, editor. Oxford: Elsevier; 2003, p. 1-17.
- [12]. McCauley JW. *Ceramic armor materials by design*. Westerville, Ohio: American Ceramic Society; 2002.
- [13]. Shokrieh MM, Javadpour GH. Penetration analysis of a projectile in ceramic composite armor. *Composite Structures* 2008;82:269-76.
- [14]. Godfrey DJ. Fabrication, formulation, mechanical properties, and oxidation of sintered Si₃N₄ ceramics using disc specimens. *Materials Science and Technology* 1985;1:510-5.
- [15]. Wagner R, Harrer W, Danzer R. Application of the Ball on Three Balls Test in the Development of a High Strength Partially Stabilised Zirconia Ceramic. *Ceramic Forum International* 2009;86:E50-E3.
- [16]. Lojanová S, Tatarko P, Chlup Z, *et al.* Rare-earth element doped Si₃N₄/SiC micro/nano-composites — RT and HT mechanical properties. *Journal of the European Ceramic Society* 2010;30:1931-44.
- [17]. Lin H-M, Jeng R-R, Lee P-Y. Microstructure and mechanical properties of vacuum hot-pressing SiC/Ti–Cu–Ni–Sn bulk metallic glass composites. *Materials Science and Engineering: A* 2008;493:246-50.
- [18]. Bolzoni L, Ruiz-Navas EM, Neubauer E, Gordo E. Inductive hot-pressing of titanium and titanium alloy powders. *Materials Chemistry and Physics* 2012;131:672-9.
- [19]. Börger A, Supancic P, Danzer R. The Ball on three Balls Test for Strength Testing of Brittle Discs - Stress Distribution in the Disc. *Journal of the European Ceramic Society* 2002;22:1425-36.
- [20]. Danzer R, Harrer W, Supancic P, *et al.* The Ball on Three Balls Test - Strength and Failure Analysis of Different Materials. *Journal of the European Ceramic Society* 2007;27:1481-5.

- [21]. Danzer R, Supancic P, Harrer W, *et al.* Biaxial Strength Testing on Mini Specimens. In: Fracture of Nano and Engineering Materials and Structures. Gdoutos EE, editor. Dordrecht: Springer; 2006, p. 589-90.
- [22]. Deluca M, Bermejo R, Pletz M, Supancic P. Strength and Fracture Analysis of Silicon Chips to be Embedded into Printed Circuit Boards. 18th European Conference on Fracture, Dresden: 2010, p. 8.
- [23]. Özkol E, Wätjen AM, Bermejo R, *et al.* Mechanical characterisation of miniaturised direct inkjet printed 3Y-TZP specimens for microelectronic applications. Journal of the European Ceramic Society 2010;30:3145-52.
- [24]. Danzer R, Supancic P, Harrer W. Der 4-Kugelversuch zur Ermittlung der biaxialen Biegefestigkeit spröder Werkstoffe. In: Technische keramische Werkstoffe. Kriegesmann J, editor. Ellerau: HvB Verlag GbR.; 2009, p. 1-48.
- [25]. Börger A, Supancic P, Danzer R. The Ball on three Balls Test for Strength Testing of Brittle Discs - Part II: Analysis of Possible Errors in the Strength Determination. Journal of the European Ceramic Society 2004;24:2917-28.
- [26]. ASTM C 1421-01b. Standard Test Methods for Determination of Fracture Toughness of Advanced Ceramics at Ambient Temperature. American Society for Testing and Materials; 2001.
- [27]. ISO 18756. Fine ceramics (advanced ceramics, advanced technical ceramics) - Determination of fracture toughness of monolithic ceramics at room temperature by the surface crack in flexure (SCF) method. 2003.
- [28]. Strobl S, Supancic P, Lube T, Danzer R. Surface crack in tension or in bending - A reassessment of the Newman and Raju formula in respect to fracture toughness measurements in brittle materials. Journal of the European Ceramic Society 2012;32:1491-501.
- [29]. Anderson TL. Fracture mechanics - fundamentals and applications. Boca Raton FL: CRC Press; 2005.
- [30]. ISO 23146. Fine ceramics (advanced ceramics, advanced technical ceramics) - Test methods for fracture toughness of monolithic ceramics - Single-edge V-notch beam (SEVNB) method. 2008.
- [31]. Rasche S, Bermejo R, Kuna M, Danzer R. Determination of Mechanical Properties of Brittle Materials by using the Small Punch Test and the Ball on three Balls Test. 18th European Conference on Fracture, Dresden: 2010.
- [32]. Supancic P. Mechanical Stability of BaTiO₃-based PTC Thermistor Components: Experimental Investigations and Theoretical Modelling. Journal of the European Ceramic Society 2000;20:2009-24.
- [33]. http://fct-keramik.de/fct/FCT-I/en/FCT_Material-Qualities.pdf. Data Sheet. 2013.
- [34]. Damani R, Gstrein R, Danzer R. Critical Notch Root Radius in SENB-S Fracture Toughness Testing. Journal of the European Ceramic Society 1996;16:695-702.
- [35]. Quinn GD, Kübler J, Gettings RJ. Fracture Toughness of Advanced Ceramics by the Surface Crack in Flexure (SCF) Method: A VAMAS Round Robin. VAMAS Report No. 17. Report 1994.
- [36]. Strobl S, Lube T, Schöppl O. Toughness measurement on ball specimens. Part II: Experimental Procedure and Measurement Uncertainties. Journal of the European Ceramic Society, 2013 (accepted).
- [37]. Strobl S, Supancic P, Lube T, Danzer R. Toughness measurement on ball specimens. Part I: Theoretical analysis. Journal of the European Ceramic Society 2012;32:1163-73.

- [38]. Börger A, Danzer R, Supancic P. Biaxial Strength Test of Discs of Different Size using the Ball on Three Balls Test. *Ceramic Engineering and Science Proceedings* 2004;25:283-9.

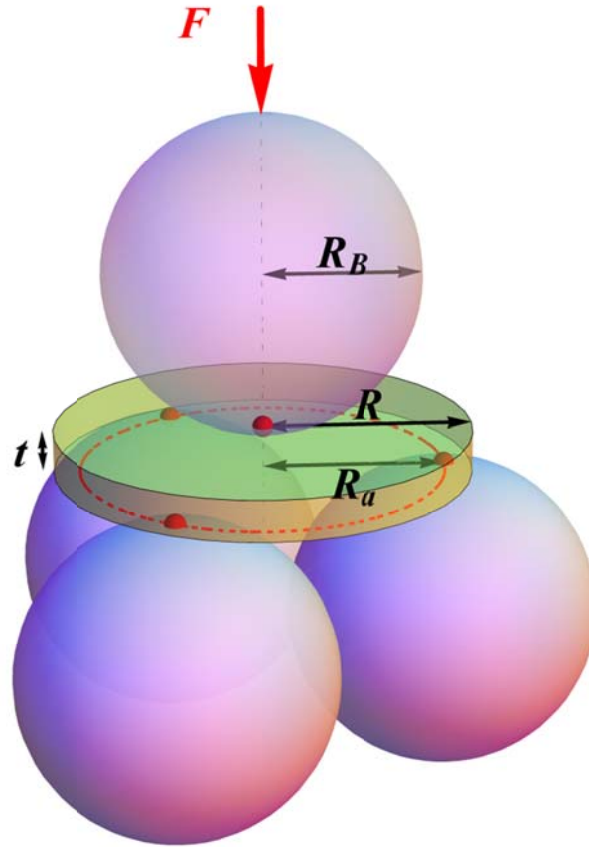


Fig. 1: Test setup of the conventional B3B strength test. In this case the test piece is a circular disc with the radius R and thickness t . The loading radius R_a is defined as the distance between the disc centre and the contact points with the supporting balls. R_a is determined by the radius of the balls R_B . The force F is applied via the centre ball, parallel to the axis of the disc (see www.isfk.at).

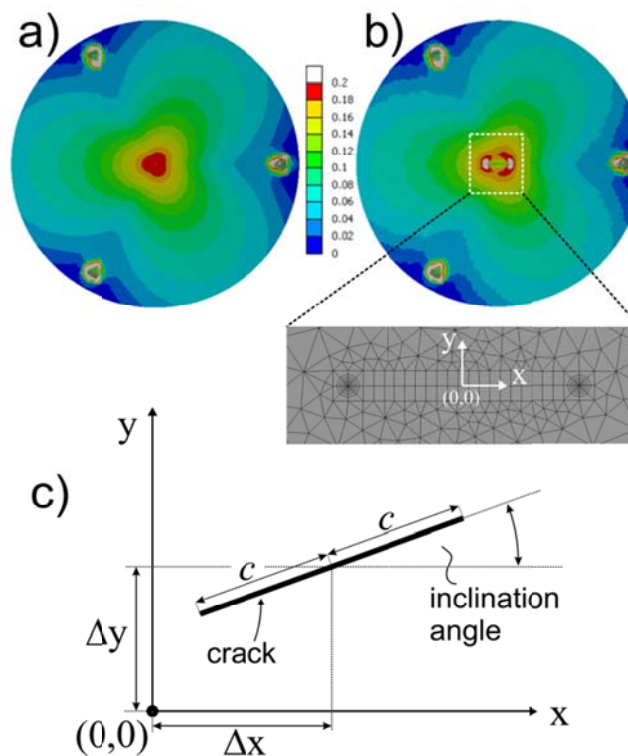


Fig. 2: View of the tensile stressed side of the B3B specimen at a load of 1 N. Plotted is the 1st principal stress in the range of 0 MPa and 0.2 MPa: a) Stress distribution of in a disc without crack and b) with surface crack and inset showing details of the crack mesh. c) sketch of possible positioning errors.

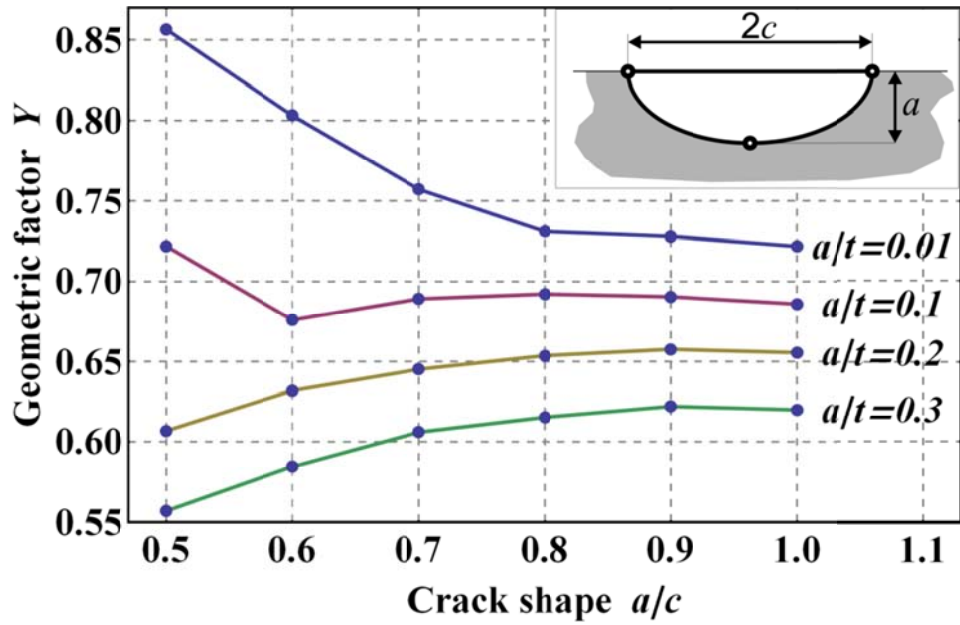


Fig. 3: Plot of the geometric factor Y as a function of the crack shape a/c and the relative crack depth a/t . In this example t/R_a is fixed to 0.3 and $\nu = 0.3$. The inset shows a sketch of the crack: a is the crack depth and $2c$ the full crack width.

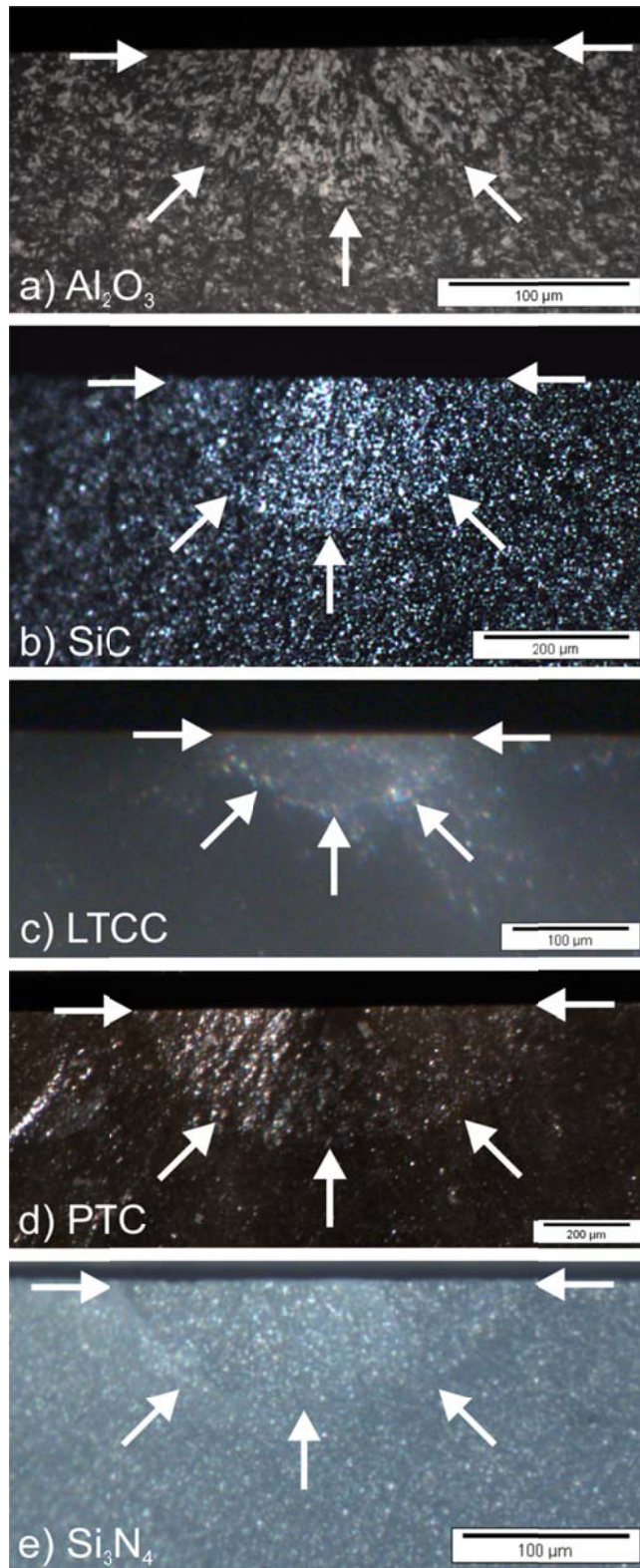


Fig. 4: Example for cracks for each investigated material.

Table 1: Specimen geometries and Poisson's ratio of the tested materials. K_{Ic} is the value determined with the B3B-KIc method. For comparison fracture toughness results of standardised methods (SEVNB and/or SCF) are given as $K_{Ic, alternative}$.

Material	R mm	R_B mm	t mm	ν -	a μm	c μm	K_{Ic} $\text{MPa m}^{1/2}$	$K_{Ic, alternative}$ $\text{MPa m}^{1/2}$
Rubalit 708S (alumina, 5)	4	2.75	0.545 ± 0.003	0.23	85 ± 7	110 ± 5	3.5 ± 0.1	3.5 ± 0.2 (SEVNB)
EKasic F (silicon carbide, 4)	10.4	7.5	2.838 ± 0.010	0.16	209 ± 10	228 ± 19	3.0 ± 0.1	2.9 ± 0.3 (SEVNB)
MKE (LTCC, 4)	10×11	4	0.799 ± 0.007	0.20	75 ± 15	140 ± 15	2.3 ± 0.2	1.9 ± 0.1 (SEVNB)
PTC (barium titanate, 11)	9.7	7.5	2.902 ± 0.080	0.29	420 ± 66	525 ± 41	1.4 ± 0.1	1.5 ± 0.1 (SCF) 1.3 ± 0.1 (SEVNB)
FSNI (silicon nitride, 5)	9.6	7.5	1.802 ± 0.012	0.27	74 ± 16	140 ± 15	5.0 ± 0.3	5.1 ± 0.2 (SCF) 5.0 ± 0.2 (SEVNB)